ACS NANO
Cite This: ACS Nano 2018, 12, 12827−12835
www.acsnano.org

ARTICLE

Self-Powered Ultraviolet Photodetector with Superhigh Photoresponsivity (3.05 A/W) Based on the GaN/Sn:Ga_2O_3 pn Junction

Daoyou Guo,[†] Yuanli Su,[†] Haoze Shi,[†] Peigang Li,[*,‡] Nie Zhao,[§] Junhao Ye,[∥] Shunli Wang,[†] Aiping Liu,[*,†] Zhengwei Chen,[‡] Chaorong Li,[†] and Weihua Tang[*,‡]

[†]Center for Optoelectronics Materials and Devices & Key Laboratory of Optical Field Manipulation of Zhejiang Province, Department of Physics, Zhejiang Sci-Tech University, Hangzhou 310018, China

[‡]Laboratory of Information Functional Materials and Devices & State Key Laboratory of Information Photonics and Optical Communications, School of Science, Beijing University of Posts and Telecommunications, Beijing 100876, China

[§]College of Materials Science and Engineering, Xiangtan University, Xiangtan 411105, Hunan Province, China

[∥]Department of Physics, Beijing Normal University, Beijing 100875, China

ABSTRACT: **Ultraviolet (UV) radiation has a variety of impacts including the health of humans, the production of crops, and the lifetime of buildings. Based on the photovoltaic effect, self-powered UV photodetectors can measure and monitor UV radiation without any power consumption. However, the current low photoelectric performance of these detectors has hindered their practical use. In our study, a super-high-performance self-powered UV photodetector based on a GaN/Sn:Ga_2O_3 pn junction was generated by depositing a Sn-doped n-type Ga_2O_3 thin film onto a p-type GaN thick film. The responsivity at 254 nm reached up to 3.05 A/W without a power supply and had a high UV/visible rejection ratio of $R_{254\ nm}/R_{400\ nm}$ = 5.9×10^3 and an ideal detectivity at 1.69×10^{13} cm·$Hz^{1/2}$·W^{-1}, which is well beyond the level of previous self-powered UV photodetectors. Moreover, our device also has a low dark current (1.8×10^{-11}A), a high I_{photo}/I_{dark} ratio (~10^4), and a fast photoresponse time of 18 ms without bias. These outstanding performance results are attributed to the rapid separation of photogenerated electron−hole pairs driven by a high built-in electric field in the interface depletion region of the GaN/Sn:Ga_2O_3 pn junction. Our results provide an improved and easy route to constructing high-performance self-powered UV photodetectors that can potentially replace traditional high-energy-consuming UV detection systems.**

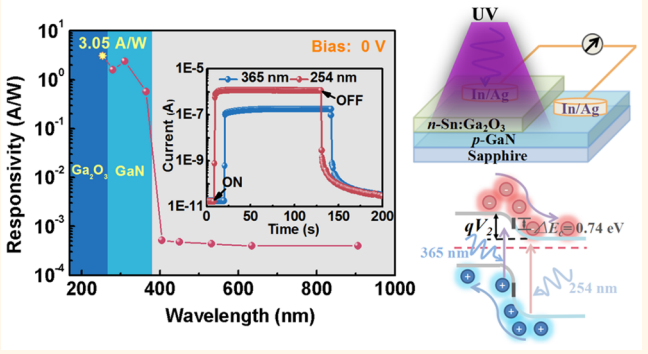

KEYWORDS: *self-powered, ultraviolet photodetector, GaN/Sn:Ga_2O_3 pn junction, superhigh photoresponsivity, 3.05 A/W, potential barrier*

Ultraviolet radiation has a significant impact on humankind. Some benefits are UV's ability to facilitate the synthesis of vitamin D, kill germs, and treat or prevent rickets when our skin is exposed to moderate UV light.[1] However, it can cause cataracts and skin cancer and accelerate the aging process due to an excessive amount of UV radiation.[1,2] Additionally, UV radiation strongly affects the production of crops and the lifetime of buildings. Fortunately, UV radiation can be measured and monitored using semiconductor UV photodetectors based on Einstein's photoelectric effect, which transforms UV radiation to measurable electronic signals. After decades of steady development, modern UV photodetectors, with high performances in photoresponsivity, signal-to-noise ratios, stability, and speed, have gained interest recently for their applications in environmental monitoring, advanced communications, air purification, leak detection, space research, *etc.*[3−13]

Unfortunately, to acquire reasonable detectivity, an external electric field is applied to photodetectors to separate the photogenerated electron−hole pairs.[5−13] Therefore, external power sources are generally necessary. This makes photodetectors overall uneconomical and complex. On the contrary, self-powered photodetectors can help solve the energy issues and have attracted significant attention.[14−19] Compared to traditional photodetectors, self-powered structures, based on the photovoltaic effect such as pn junctions, heterojunctions,

Received: October 19, 2018
Accepted: November 28, 2018
Published: November 28, 2018

DOI: 10.1021/acsnano.8b07997
ACS Nano 2018, 12, 12827−12835

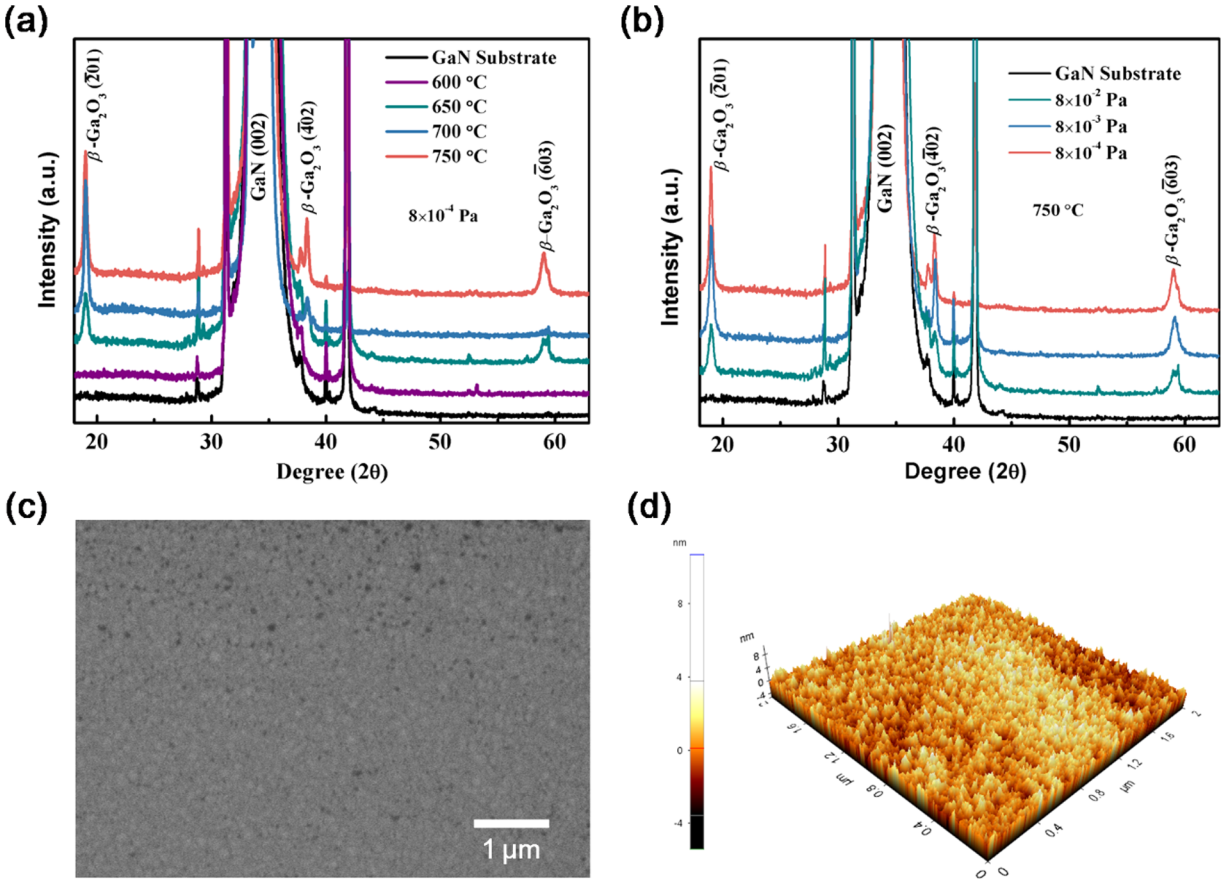

Figure 1. XRD patterns of Sn:Ga_2O_3 thin films deposited on a GaN film substrate at different (a) substrate temperatures and (b) oxygen pressures. (c) FE-SEM plane-view and (d) AFM images of the surface morphology for Sn:Ga_2O_3 thin films deposited on a GaN film at 8 × 10^{-4} Pa and 750 °C.

Schottky junctions, and organic/inorganic hybrid junctions, separate the electron−hole pairs rapidly with the built-in electric field.[20] This reveals a higher photosensitivity and faster photoresponse at zero bias without consuming external power.[14−21] Self-powered UV photodetectors have great application potential. They not only are used to detect humidity and toxic gas sensitivity but also function as batteries or hybrid supercapacitors.[1]

For self-powered UV photodetectors, the photoresponsivities are still low for practical applications even though great progress has been made in recent years.[1] Shen *et al.* fabricated self-powered UV photodetectors using an n-ZnO/p-NiO core−shell nanowire array heterojunction and a Au/β-Ga_2O_3 nanowire array film Schottky junction with responsivities of 0.49 and 0.01 mA/W, respectively.[14,21] Fang *et al.* prepared a highly crystalline individual ZnO−Ga_2O_3 core−shell heterojunction, which shows a responsivity of 9.7 mA/W at 251 nm under zero bias.[15] Zheng *et al.* first constructed a back-to-back p-graphene/AlN/p-GaN vacuum ultraviolet photovoltaic detector, which exhibits a responsivity of 67 mA/W and an extremely fast response of 80 ns at 0 V.[11] In previous work, our group constructed a heterojunction based on Ga_2O_3/NSTO,[22] Ga_2O_3/Ga:ZnO,[17] and p-GaN/n-Ga_2O_3[23] for self-powered UV photodetectors, which exhibits responsivities of 2.6 mA/W (254 nm), 0.763 mA/W (254 nm), and 54.43 mA/W (365 nm), respectively. Among these photodetectors, the pn junction based on the GaN/Ga_2O_3 heterojunction with a suitable energy band potential barrier led to innovation for the next generation of self-powered UV photodetectors. The p-type GaN thin film layer can be obtained easily by doping Mg.[24,25] β-Ga_2O_3 shows an intrinsic n-type semiconductor due to oxygen deficiency.[26−29] To engineer high-performance GaN/Ga_2O_3-based self-powered UV photodetectors, it is crucial to understand the physical mechanisms. The photogenerated carriers need to be separated by the built-in potential between GaN and Ga_2O_3; therefore an energy band structure with a large built-in electric field is essential. In our previous paper, we used the intrinsic Ga_2O_3 acting as n-type.[23] If β-Ga_2O_3 is doped with tetravalent elements, the Fermi level will move close to the conduction band. As a result, the built-in potential barrier will be larger and the separation of the photogenerated carriers will be more effective and fast. Herein, the pn junctions based on GaN/Sn-doped Ga_2O_3 (GaN/Sn:Ga_2O_3) are constructed by depositing Sn:Ga_2O_3 thin films on p-type GaN films. The GaN/Sn:Ga_2O_3 junction shows a superhigh photoresponsivity of 3.05 A/W under 254 nm UV light and under zero bias. This exhibits applications for communication and space detection.

RESULTS AND DISCUSSION

The p-type Mg:GaN thin films have a band gap of 3.38 eV and are sensitive to UV light at wavelengths less than 367 nm.[23] Various substrate temperatures and oxygen pressures were explored to grow a Sn:Ga_2O_3 thin film. The X-ray diffraction (XRD) patterns of GaN/Sn:Ga_2O_3 pn junctions prepared at different growth conditions are shown in Figure 1(a) and (b).

DOI: 10.1021/acsnano.8b07997
ACS Nano 2018, 12, 12827−12835

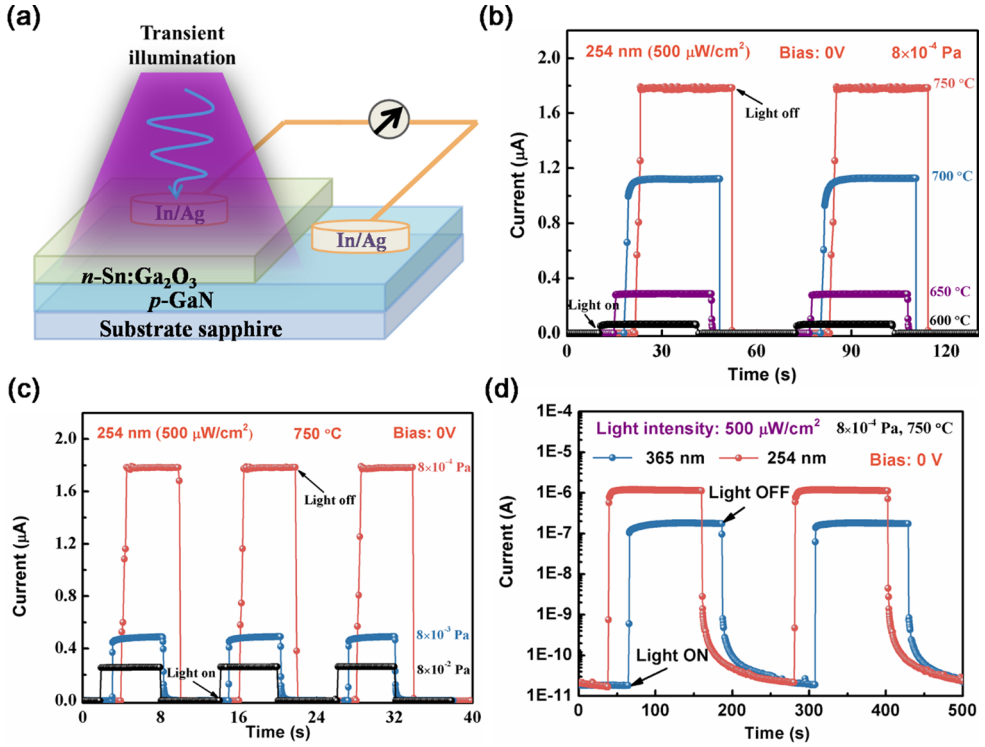

Figure 2. (a) Schematic illustration of the fabricated prototype GaN/Sn:Ga_2O_3 pn junction photodetector; time-dependent photoresponse of the GaN/Sn:Ga_2O_3 pn junction photodetector with the Sn:Ga_2O_3 thin films grown under different (b) substrate temperatures and (c) oxygen pressures by periodically turning on and off the 254 nm UV illumination (with a light intensity of 500 μW/cm^2) at zero bias. (d) Time-dependent photoresponse of the GaN/Sn:Ga_2O_3 pn junction photodetector with the Sn:Ga_2O_3 thin films grown at 8 × 10^{-4} Pa and 750 °C by periodically turning on and off the 365 and 254 nm UV illumination with a light intensity of 500 μW/cm^2 at zero bias.

No peaks relating to Ga_2O_3 were observed in the XRD pattern of the film deposited at 600 °C. There were, however, peaks corresponding to the substrate. As shown in Figure 1(a), the XRD pattern exhibited an amorphous structure, possibly due to the lack of kinetic energy for the formation of β-Ga_2O_3 films.[27] At a substrate temperature of 650 °C, the thin film starts to crystallize with the presence of three peaks located at 18.83°, 38.17°, and 58.86°, respectively, which corresponds to the $(\bar{2}01)$ and higher order diffraction lattice plane of β-Ga_2O_3.[30] The crystallization quality of β-Ga_2O_3 thin films improves as the substrate temperature increases up to 750 °C under the fixed oxygen pressure of 8 × 10^{-4} Pa [Figure 1(a)]. With an increase of oxygen pressure, the peak intensities of $(\bar{2}01)$ and higher order diffraction lattice planes from Ga_2O_3 decrease at the substrate temperature of 750 °C [Figure 1(b)]. Comparing the growth conditions above, the thin films prepared at 8 × 10^{-4} Pa and 750 °C have a better crystallization with an out-of-plane relationship of β-Ga_2O_3 $(\bar{2}01)$ parallel to GaN (002). Figure 1(c) shows the plane-view image of the Sn:Ga_2O_3 thin films deposited on a Mg:GaN film substrate at a pressure of 8 × 10^{-4} Pa and a temperature of 750 °C using a field emission scanning electron microscope (FE-SEM). Figure 1(d) shows the surface morphology of the thin film obtained using an atomic force microscope (AFM) with a scanning area of 2 × 2 μm. The root-mean-square (RMS) surface roughness obtained is 4.76 nm.

The contacts between the In/Ag electrodes and GaN or Ga_2O_3 thin films are ohmic and have been investigated and given in our previous work.[23] Figure 2(a) displays a schematic illustration of the fabricated prototype heterojunction photodetector. The UV photoelectric properties of GaN/Sn:Ga_2O_3 pn junctions prepared under various substrate temperatures and oxygen pressures are measured. Figure 2(b) and (c) show the time-dependent photoresponse by intermittently turning on and off the 254 nm UV illumination with an intensity of 500 μW/cm^2 under an applied bias of 0 V. The photocurrent increases as the substrate temperature increases from 600 °C up to 750 °C under a fixed oxygen pressure of 8 × 10^{-4} Pa. However, the photocurrent decreases as the oxygen pressure increases at a fixed substrate temperature of 750 °C. As a result, the GaN/Sn:Ga_2O_3 pn junction photodetector with the Sn:Ga_2O_3 thin films grown under an oxygen pressure of 8 × 10^{-4} Pa and a substrate temperature of 750 °C exhibits the best photocurrent. All of the following investigations are performed based on the above growth conditions.

Figure 2(d) shows the time-dependent photoresponse by intermittently switching on and off the 365 and 254 nm UV illumination. The intensities for both UV radiations are 500 μW/cm^2 under zero bias. The dark current is approximately 1.8 × 10^{-11} A. When the 365 nm UV light was turned on, the current detected increases instantly to 1.7 × 10^{-7} A, with the ratio of I_{photo}/I_{dark} being approximately 4 orders of magnitude ($\sim 10^4$), exhibiting the characteristic of being self-powered. When the UV light is turned off, the current drops to the dark count. For the 254 nm UV light, the I_{photo}/I_{dark} ratio of the GaN/Sn:Ga_2O_3 pn junction photodetector is about 6.1 × 10^4 with a photocurrent of 1.1 × 10^{-6} A.

These results show that the photodetector based on GaN/Sn:Ga_2O_3 pn junction functions without an external power supply. The zero power consumption observed is attributed to the photovoltaic properties of the pn junction between GaN and Sn:Ga_2O_3, as shown in Figure 3. The I–V curve of the

DOI: 10.1021/acsnano.8b07997
ACS Nano 2018, 12, 12827–12835

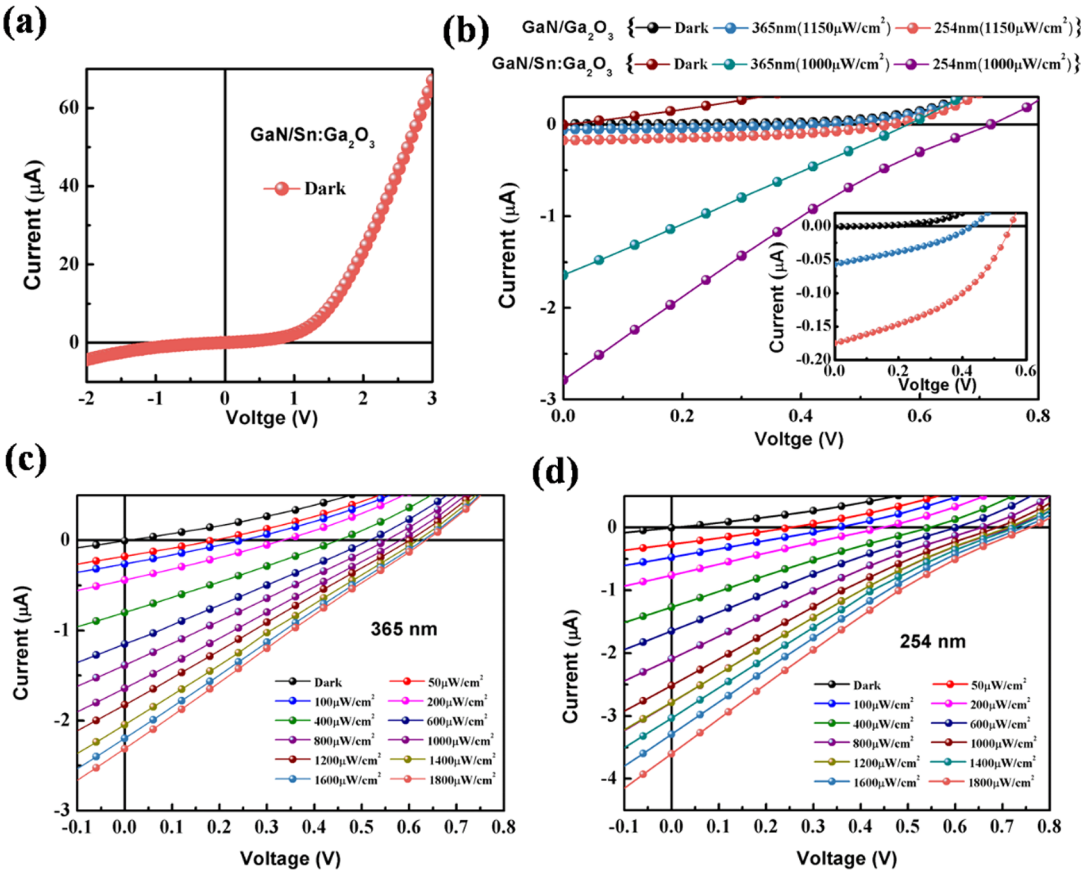

Figure 3. (a) *I*–*V* characteristic curve of the GaN/Sn:Ga_2O_3 pn junction photodetector in the dark;. (b) Comparison of the *I*–*V* enlarged curves near zero bias between the GaN/Ga_2O_3 pn junction photodetector and the Sn doping GaN/Sn:Ga_2O_3 pn junction photodetector in the dark, at 365 and 254 nm illumination; *I*–*V* curves of the GaN/Sn:Ga_2O_3 pn junction photodetector with the Sn:Ga_2O_3 thin films grown at 8 × 10^{-4} Pa and 750 °C in the dark at (c) 365 nm and (d) 254 nm illumination with various light intensities.

GaN/Sn:Ga_2O_3 pn junction presents typical rectifying characteristics (Figure 3(a)), which is similar to that of the GaN/Ga_2O_3 pn junction, indicating that the GaN/Sn:Ga_2O_3 junction functions as a well-defined diode. In solar cells, when the negative photocurrent under voltage reaches zero, it is called a short-circuit current, which is due to the generation and collection of light-generated carriers. The short-circuit current is an important parameter for solar cells. Compared to the GaN/Ga_2O_3 junction, the Sn doping GaN/Sn:Ga_2O_3 pn junction photodetector exhibits a large enhanced short-circuit current, which is depicted in Figure 3(b). When the intensity of the illumination reaches 1150 μW/cm^2, the short-circuit current of the GaN/Ga_2O_3 pn junction photodetector is 0.175 and 0.058 μA at 365 and 254 nm UV illuminations, respectively (inset panel of Figure 3(b)). When the intensity of the illumination is 1000 μW/cm^2, the short-circuit currents of the GaN/Sn:Ga_2O_3 pn junction photodetector are 1.641 and 2.785 μA at 365 and 254 nm illuminations, respectively. When the thin film is illuminated with 254 nm UV light, the short-circuit current is enhanced 48 times for the Sn-doped Ga_2O_3 thin film. One advantage of this device is that it does not need an external power source; the photodetector generates a nonequilibrium carrier through radiation. Figure 3(c) and (d) show the enlarged current (*I*) *versus* voltage (*V*) properties of the GaN/Sn:Ga_2O_3 pn junction photodetector at 365 and 254 nm UV light under various light intensities, respectively, at zero bias. In the dark, the *I*–*V* curve passes through the origin of the coordinate. When the photodetector is exposed to 254 or 365 nm UV light, the *I*–*V* curve deviates from the coordinate origin and exhibits a negative photocurrent under zero bias. Under the illumination of a fixed light intensity, the short-circuit current increases concomitantly with increased intensity of illumination. At a light intensity of 1800 μW/cm^2, the short-circuit current values are 2.3 and 3.6 μA at 365 and 254 nm UV light, respectively. The intensity of the radiation is detected by measuring the photoelectric voltage or current. The results from above show that a GaN/Sn:Ga_2O_3 pn junction photodetector can function without an external power source, making it therefore a self-powered device, which has potentially important applications such as secure ultraviolet communication and space detection.

As shown in Figure 4(a), the continuous time-dependent photoresponse cycles of the photodetector have a nearly identical response under 254 nm light and 365 nm light illumination with a light intensity of 1000 μW/cm^2 and at zero bias, showing high robustness and good reproducibility. A measurement under 254 nm UV light illumination with an intensity ranging from 50 to 1800 μW/cm^2 was used to evaluate the influence of intensity on the response of the photodetector (Figure 4(b)). Figure 4(c) shows the photocurrent and responsivity of the photodetector as a function of the intensity of illuminating light. The photocurrent increases almost linearly as the intensity of the illumination increases. A higher light intensity would produce more photogenerated electron–hole pairs, resulting in a higher photocurrent. Responsivity (*R*), a photodetector parameter to evaluate

DOI: 10.1021/acsnano.8b07997
ACS Nano 2018, 12, 12827–12835

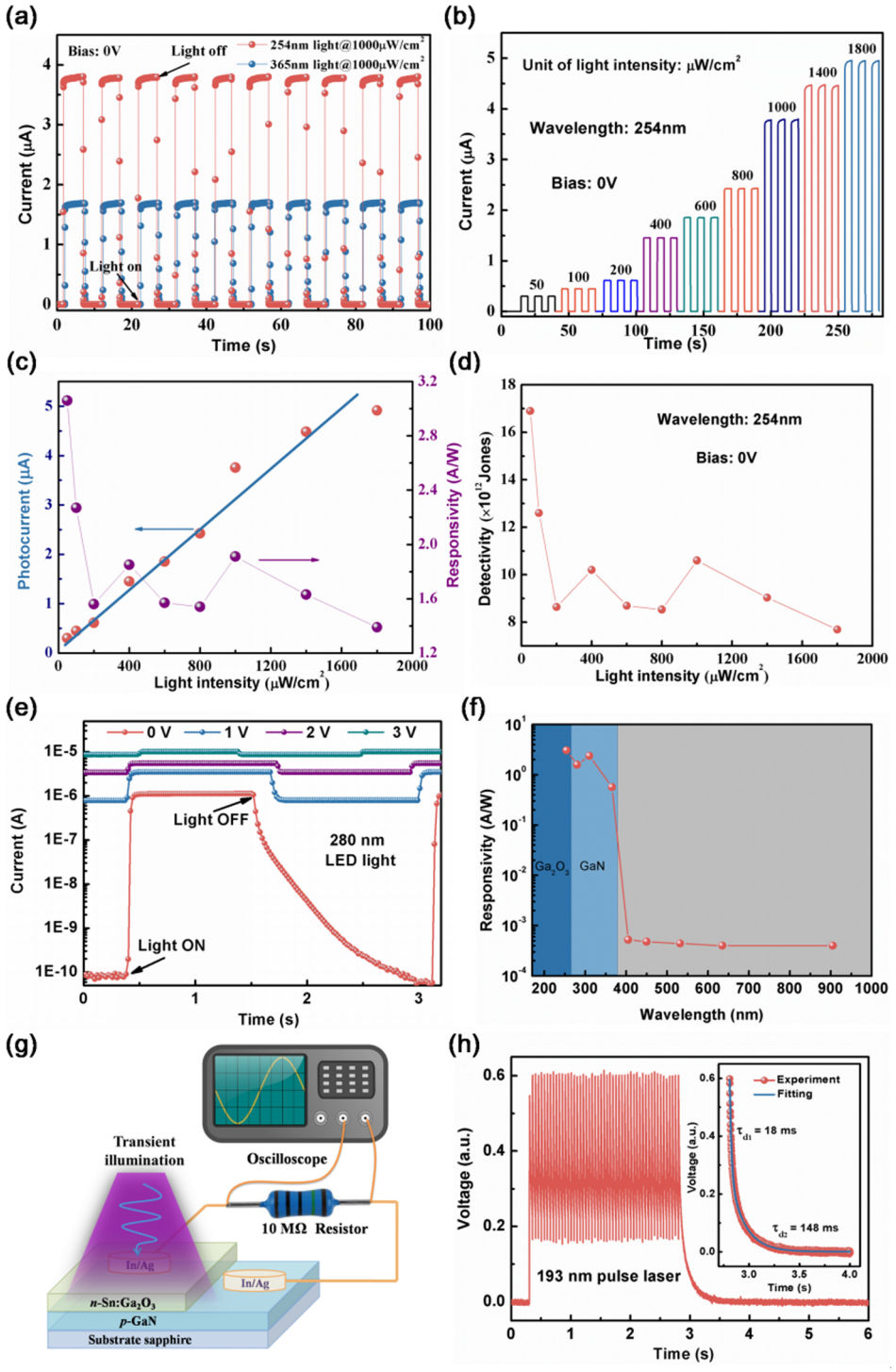

Figure 4. (a) Continuous time-dependent photoresponse of the GaN/Sn:Ga_2O_3 pn junction photodetector under zero bias at 254 and 365 nm illumination with a light intensity of 1000 μW/cm^2. (b) Time-dependent photoresponse of the photodetector under zero bias and 254 nm light with various light intensities. (c) Photocurrent and responsivity as a function of the light intensity. (d) Detectivity as a function of the light intensity. (e) Time-dependent photoresponse of the photodetector under various bias with 280 nm LED light illumination. (f) Wavelength selectivity of the photodetector under zero bias. (g) Photoresponse measurement configuration of the GaN/Sn:Ga_2O_3 pn junction photodetector. (h) Temporal pulse photoresponse of the photodetector excited by a 193 nm pulse laser for 50 pulses; (inset) enlarged view of the decay edge and the corresponding exponential fitting.

sensitivity, was calculated as previously shown by the following formula: $R = (I_{photo} - I_{dark})/(PS)$, where I_{photo} is the photocurrent, I_{dark} is the dark current, P is the supplied light intensity, and S is the effective area of the photodetector.[31,32] In summary, the responsivity decreases as the light intensity increases. When more electron−hole pairs are generated with a higher light intensity, self-heating will be induced, which not only increases charge carrier scattering but also increases the possibility of recombination. At 254 nm UV illumination with an intensity of 50 μW/cm^2, a maximum R of 3.05 A/W was

DOI: 10.1021/acsnano.8b07997
ACS Nano 2018, 12, 12827−12835

Table 1. Comparison of the Photoresponse Parameters of the GaN/Sn:Ga_2O_3 pn Junction UV Photodetector under Zero Bias from This Work and Other Previously Reported Self-Powered Devices

photodetector	wavelength (nm)	responsivity (mA/W)	$R_{peak}/R_{400\ nm}$ rejection ratio	I_{photo}/I_{dark} rejection ratio	rise time/decay time	detectivity [Jones]	ref
Au/Ga_2O_3	258	0.01	38		1 μs/100 μs		13
diamond/β-Ga_2O_3	244	0.2	135	37			3
Ga_2O_3/NSTO	254	2.6		20	0.21 s/0.07 s		20
polyaniline/MgZnO	250	0.16	$\sim 10^4$		<0.3 s/<0.3 s	1.5×10^{11}	32
GaN/ZnO	358	0.68					34
n-ZnO/p-NiO	370	0.493			1.38 μs/10 μs		20
Ag/ZnMgO/ZnO	275	16	$\sim 10^4$		24 μs/300 μs	5×10^9	35
ZnO/Ga_2O_3	251	9.7	6.9×10^2		100 μs/900 μs	6.3×10^{12}	14
GaN/Ga_2O_3	254	28.44		80	0.14 s/0.07 s	6.2×10^{10}	22
GaN/Sn:Ga_2O_3	254	3.05×10^3	5.9×10^3	6.1×10^4	0.018s	1.69×10^{13}	this work

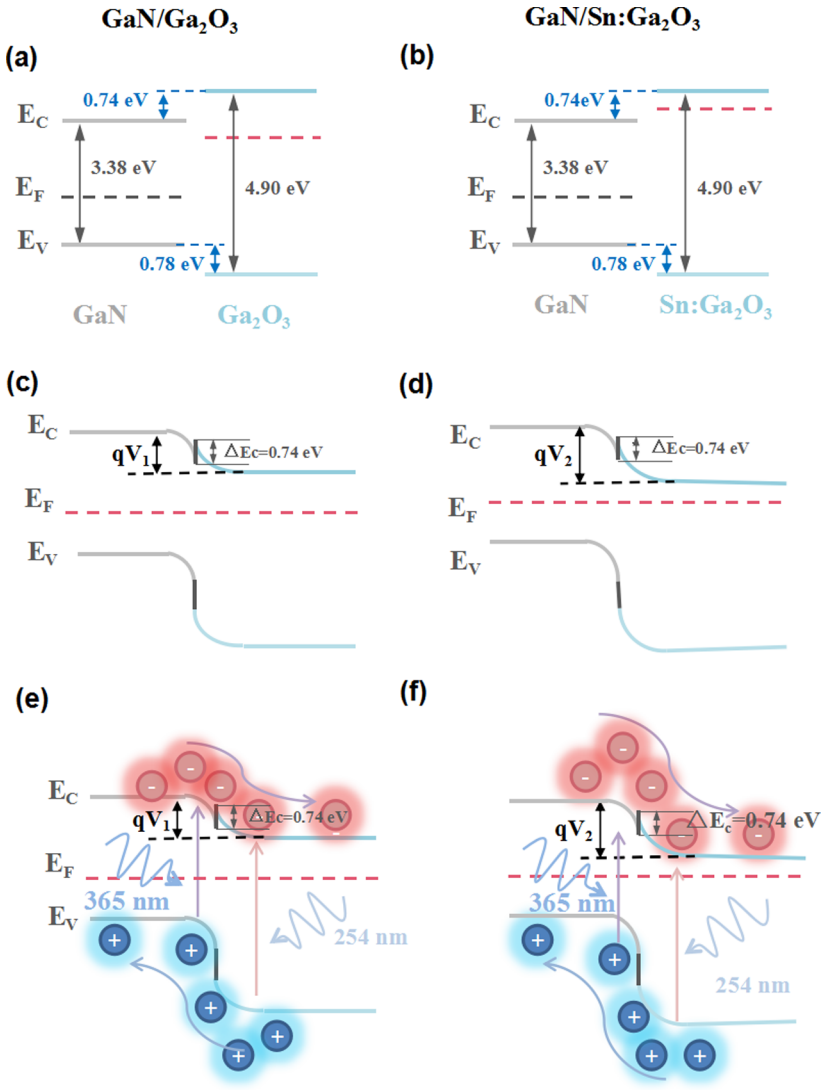

Figure 5. Schematic energy band diagrams of the GaN/Ga_2O_3 and GaN/Sn:Ga_2O_3 pn junctions: (a, b) before contact; (c, d) dark conditions (after contact); (e, f) at 254 and 365 nm UV illumination (after contact), respectively.

obtained for the GaN/Sn:Ga_2O_3 pn junction photodetector. Currently, this is the highest reported value for self-powered UV photodetectors under zero bias. The detectivity (D) is a figure-of-merit of a photodetector, which usually describes the smallest detectable signal.[33,34] The D of the GaN/Sn:Ga_2O_3 photodetector can be calculated using the calculation $D = R/(2eJ)^{1/2}$ as previously described, where e is the elemental charge and J is the dark current density.[34,35] The parameter D of the photodetector decreases as the light intensity increases and has a similar trend in responsivity, as shown in Figure 4(d). A maximum value of D of 1.69×10^{13} cm·$Hz^{1/2}$·W^{-1} was

DOI: 10.1021/acsnano.8b07997
ACS Nano 2018, 12, 12827−12835

obtained under 50 μW/cm^2 254 nm light illumination at zero bias, which reveals a high signal-to-noise ratio.

The influence of applied biases on the photoresponses of the GaN/Sn:Ga_2O_3 pn junction photodetector was also investigated under 280 nm LED light illumination (Figure 4(e)). The dark current (I_{dark}) increases rapidly from about 9.0 × 10^{-11} A to 2.1× 10^{-7} A as the voltage jumps from 0 to 0.5 V, and then I_{dark} increases steadily as the voltage increases. Both I_{dark} and I_{photo} increase as the applied bias increases. The dark current increases when a higher bias is applied due to the faster drift velocity and the release of more carriers from oxygen vacancy traps. A higher photocurrent corresponds to higher bias, which can be attributed to an increase in photogenerated electron−hole pair separation. The ratio of I_{dark}/I_{photo} decreases as the bias increases. The ratios at different biases are 1.2 × 10^4, 11.9, 4.5, 2.3, 1.6, 1.3, and 1.1 at 0, 0.5, 1, 1.5, 2, 2.5, and 3 V, respectively.

The wavelength-dependent photoresponsivity of the GaN/Sn:Ga_2O_3 pn junction photodetector under zero bias was evaluated with LED illumination at wavelengths of 254, 280, 310, 365, 400, 450, 532, 635, and 905 nm. The results are shown in Figure 4(f). A maximum R of 3.05 A/W was obtained at 254 nm, which corresponds to the band gap of Ga_2O_3 (4.9 eV), implying that the photodetector presents an extremely high detectivity to weak solar-blind UV signals. The R exhibits a sharp jump between 365 nm ($R_{365\ nm}$ = 0.57 A/W) and 400 nm ($R_{400\ nm}$ = 5.2 × 10^{-4} A/W) light, which indicates that the self-powered photodetector is a UV photodetector. The UV/visible rejection ratio ($R_{254\ nm}/R_{400\ nm}$) of our GaN/Sn:Ga_2O_3 pn junction photodetector is about 5.9 × 10^3, which represents high spectral selectivity of the UV region.

Furthermore, a special measurement system (Figure 4(g)) is constructed for fast-speed photon detection.[36] A 100 MΩ load resistor is in series with the GaN/Sn:Ga_2O_3 pn junction photodetector.[36] An oscilloscope records the bias change of the load resistor and monitors the current variation of the series circuit. Figure 4(h) shows the temporal pulse photoresponse of the photodetector continuously excited by a 193 nm pulse laser for 50 pulses. The dynamic response of the photodetector presents good stability and reproducibility. The photoresponse decay curve was fitted using a biexponential relaxation equation, $I = I_0 + Ce^{-t/\tau_1} + De^{-t/\tau_2}$, where I_0 stands for the steady state photocurrent, t represents the time, C and D are constants, and τ_1 and τ_2 are relaxation time constants.[10,22] The inset of Figure 4(h) shows that the decay process is well fitted. The decay process consists of a fast-response component and a slow-response component, corresponding to a τ_{d1} of 18 ms and a τ_{d2} of 148 ms. Usually, the fast-response component is due to the rapid change of carrier concentration when the light is turned on/off; the slow-response component is due to the carrier trapping/releasing from defects.[6]

Comparison of the photoresponse parameters under zero bias of the GaN/Sn:Ga_2O_3 pn junction UV photodetector in this work and other previously reported self-powered devices is listed in Table 1.[37,38] The GaN/Sn:Ga_2O_3 pn junction heterojunction UV photodetector shows a larger responsivity, detecivity, and I_{photo}/I_{dark} ratio than those of other UV self-powered photodetectors. The UV/visible rejection ratio and photoresponse speed are comparable to those of the previously reported UV self-powered photodetectors.

Compared to the GaN/Ga_2O_3 junction, the GaN/Sn:Ga_2O_3 pn junction photodetector has improved substantially. In order to explain the microscopic photoinduced electrical conduction mechanism, energy band diagrams of the GaN/Ga_2O_3 and GaN/Sn:Ga_2O_3 heterojunctions are given in Figure 5. According to our previous work,[23] the band gap of GaN and Ga_2O_3 are 3.38 and 4.9 eV, respectively, and the valence band maximum are 1.58 and 4.05 eV, respectively. Thus, the valence band offset ΔE_V = 0.78 eV and the conduction band offset ΔE_c = 0.74 eV of the GaN/Ga_2O_3 heterojunction can be calculated. Figure 5(a) shows the diagram of the energy band of the GaN/Ga_2O_3 heterojunction. After contact, carriers can flow until both Fermi levels line up, and a pn junction depletion layer is formed near the interface of GaN/Ga_2O_3. The built-in potential barrier (qV) of the pn junction can be calculated using the difference between the work functions of GaN and Ga_2O_3. For the self-powered photodetector, the built-in potential barrier is the most important factor because the photogenerated carriers are separated only by the electric field under zero bias. The larger the value of qV, the better performance a photodetector has. Because the Fermi level of Sn-doped Ga_2O_3 is closer to the conduction band than that of pure Ga_2O_3 due to more free carriers (Figure 5(b)), the built-in potential barrier of the GaN/Sn:Ga_2O_3 junction (qV_2) is larger than that of the GaN/Ga_2O_3 junction (qV_1), as shown in Figure 5(c) and (d). When UV light irradiates the device, the light penetrates the electrode into the interface of the GaN/Ga_2O_3 heterojunction and generates electron−hole pairs. Under zero bias, the photogenerated electron−hole pairs in the depletion layer rapidly separate under the built-in electric field. The electrons transport toward n-type Ga_2O_3; the holes transport toward p-type GaN and then toward corresponding electrodes (Figure 5(e) and (f)). The Ga_2O_3 thin film is used as the window for penetrating UV light, and the n-type semiconductor for constructing the pn junction. The core workspace of the pn junction self-powered photodetectors is the depletion layer. The separation of the photogenerated carriers is more effective and faster with a larger built-in potential barrier. As a result, the GaN/Sn:Ga_2O_3 pn junction photodetector exhibits a better self-powered performance than the GaN/Sn:Ga_2O_3 photodetector.

CONCLUSIONS

In summary, the self-powered UV photodetectors were successfully built with a GaN/Ga_2O_3 pn junction through depositing an n-type Ga_2O_3 thin film onto an Al_2O_3 single-crystal substrate shielded by a p-type GaN thin film. Compared to the pure Ga_2O_3 film, the photoresponse of the GaN/Ga_2O_3 pn junction photodetectors based on Sn-doped Ga_2O_3 thin films has improved. The responsivity at 254 nm can reach up to 3.05 A/W with a high UV/visible rejection ratio ($R_{254\ nm}/R_{400\ nm}$ = 5.9 × 10^3) under zero bias. Additionally, the device exhibits a low dark current (1.8 × 10^{-11}A), a high I_{photo}/I_{dark} ratio (~10^4), an excellent detectivity rate (1.69 × 10^{13} cm·$Hz^{1/2}$·W^{-1}), and a fast photoresponse time (18 ms). These improvements are attributed to the rapid separation of photogenerated electron−hole pairs driven by a built-in electric field in the interface depletion region of the GaN/Sn:Ga_2O_3 pn junction. The results reported in this study show the construction of a high-responsivity self-powered UV photodetector with potential applications in environmental monitoring, insecure communication, and space detection.

DOI: 10.1021/acsnano.8b07997
ACS Nano 2018, 12, 12827−12835

METHODS

Preparation and Characterization of Materials. The p-type Mg-doped GaN (Mg:GaN) thin films with a thickness of 4 μm grown on *c*-plane (0001) Al_2O_3 were used as substrates (purchased from Suzhou Nanowin Science and Technology Co. Ltd.). The carrier mobility of GaN thin films is about 10 $cm^2\ V^{-1}\ s^{-1}$. The n-type Sn-doped Ga_2O_3 thin film with a thickness of 375 nm was deposited on the GaN film by pulse laser deposition (PLD). A Ga_2O_3 ceramic disk with a Sn doping concentration of 2 at. % was used as the target. The chamber base pressure was 1×10^{-6} Pa. Optimal growth conditions were explored by ranging the temperature of the film growth from 600 to 750 °C and the oxygen pressure from 8×10^{-4} to 8×10^{-2} Pa. The laser ablation was performed using a 248 nm KrF excimer laser at a fluence of 4 J/cm^2 with a repetition rate of 2 Hz. A detailed preparation is described in early work.[23] The structure, crystallinity, and orientation of the as-grown thin films were characterized by XRD. The surface morphology was characterized by an FE-SEM and a Bruker-Veeco AFM.

Performance Test of Devices. For the performance test of the UV photodetector, Ag circular electrodes (0.5 mm diameter) with a thickness of 7 nm were deposited on both sides, the Sn:Ga_2O_3 thin film surface and the GaN film surface, respectively, as a semi-transparent electrode through a metal mask by radio frequency magnetron sputtering. A small point electrode (~0.1 mm diameter) of In metal was pressed onto the Ag circular electrode to obtain a region to connect Cu wires. A Keithley 4200 was used to measure the current−voltage (*I*−*V*) characteristics and time-dependent photoresponse of the fabricated device. The time-dependent photoresponse measurement was carried out through the use of a low-pressure mercury lamp at 254 nm with varying light intensities and applied biases. All experiments were performed at room temperature.

AUTHOR INFORMATION

Corresponding Authors

*E-mail: pgli@bupt.edu.cn.
*E-mail: liuaiping1979@gmail.com.
*E-mail: whtang@bupt.edu.cn.

ORCID

Daoyou Guo: 0000-0002-6191-1655
Nie Zhao: 0000-0002-3824-9974

Notes

The authors declare no competing financial interest.

ACKNOWLEDGMENTS

The authors thank Prof. Feng Huang, Dr. Wei Zheng, and Dr. Richeng Lin from the School of Materials at Sun Yat-sen University for the spectral photoresponse and temporal pulse photoresponse measurements. This work was supported by the National Natural Science Foundation of China (Nos. 61704153, 51572241, 61774019, 51572033, 11605149), Zhejiang Public Service Technology Research Program/Analytical Test (LGC19F040001), Open Fund of IPOC (BUPT), Beijing Municipal Commission of Science and Technology (SX2018-04), Nature Science Foundation of Hunan Province (2017JJ3309), and Scientific Research Project for the Education Department of Zhejiang Province (Y201738294).

REFERENCES

(1) Chen, H.; Liu, K.; Hu, L.; Al-Ghamdi, A. A.; Fang, X. New Concept Ultraviolet Photodetectors. *Mater. Today* **2015**, *18*, 493−502.

(2) Teng, F.; Hu, K.; Ouyang, W.; Fang, X. Photoelectric Detectors Based on Inorganic *p*-Type Semiconductor Materials. *Adv. Mater.* **2018**, *30*, 1706262.

(3) Chen, Y. C.; Lu, Y. J.; Lin, C. N.; Tian, Y. Z.; Gao, C. J.; Dong, L.; Shan, C. X. Self-Powered Diamond/β-Ga_2O_3 Photodetectors for Solar-Blind Imaging. *J. Mater. Chem. C* **2018**, *6*, 5727−5732.

(4) Guo, D. Y.; Shi, H. Z.; Qian, Y. P.; Lv, M.; Li, P. G.; Su, Y. L.; Liu, Q.; Chen, K.; Wang, S. L.; Cui, C.; Li, C. R.; Tang, W. H. Fabrication of β-Ga_2O_3/ZnO Heterojunction for Solar-Blind Deep Ultraviolet Photodetection. *Semicond. Sci. Technol.* **2017**, *32*, 03LT01.

(5) Chu, J. W.; Wang, F. M.; Yin, L.; Lei, L.; Yan, C. Y.; Wang, F.; Wen, Y.; Wang, Z. X.; Jiang, C.; Feng, L. P.; Xiong, J.; Li, Y. R.; He, J. High-Performance Ultraviolet Photodetector Based on a Few-Layered 2D $NiPS_3$ Nanosheet. *Adv. Funct. Mater.* **2017**, *27*, 1701342.

(6) Guo, D. Y.; Wu, Z. P.; An, Y. H.; Guo, X. C.; Chu, X. L.; Sun, C. L.; Li, L. H.; Li, P. G.; Tang, W. H. Oxygen Vacancy Tuned Ohmic-Schottky Conversion for Enhanced Performance in β-Ga_2O_3 Solar-Blind Ultraviolet Photodetectors. *Appl. Phys. Lett.* **2014**, *105*, 023507.

(7) Lin, R.; Zheng, W.; Zhang, D.; Zhang, Z.; Liao, Q.; Yang, L.; Huang, F. High-Performance Graphene/β-Ga_2O_3 Heterojunction Deep-Ultraviolet Photodetector with Hot-Electron Excited Carrier Multiplication. *ACS Appl. Mater. Interfaces* **2018**, *10*, 22419−22426.

(8) Cui, S.; Mei, Z.; Zhang, Y.; Liang, H.; Du, X. Room-Temperature Fabricated Amorphous Ga_2O_3 High-Response-Speed Solar-Blind Photodetector on Rigid and Flexible Substrates. *Adv. Opt. Mater.* **2017**, *5*, 1700454.

(9) Li, Y.; Tokizono, T.; Liao, M.; Zhong, M.; Koide, Y.; Yamada, I.; Delaunay, J.-J. Efficient Assembly of Bridged β-Ga_2O_3 Nanowires for Solar-Blind Photodetection. *Adv. Funct. Mater.* **2010**, *20*, 3972−3978.

(10) Guo, D. Y.; Wu, Z. P.; Li, P. G.; An, Y. H.; Liu, H.; Guo, X. C.; Yan, H.; Wang, G. F.; Sun, C. L.; Li, L. H.; Tang, W. H. Fabrication of β-Ga_2O_3 Thin Films and Solar-Blind Photodetectors by Laser MBE Technology. *Opt. Mater. Express* **2014**, *4*, 1067−1076.

(11) Zheng, W.; Lin, R.; Ran, J.; Zhang, Z.; Ji, X.; Huang, F. Vacuum-Ultraviolet Photovoltaic Detector. *ACS Nano* **2018**, *12*, 425−431.

(12) Zheng, W.; Lin, R.; Zhu, Y.; Zhang, Z.; Ji, X.; Huang, F. Vacuum Ultraviolet Photodetection in Two-Dimensional Oxides. *ACS Appl. Mater. Interfaces* **2018**, *10*, 20696−20702.

(13) Luo, J. J.; Li, S. R.; Wu, H. D.; Zhou, Y.; Li, Y.; Liu, J.; Li, J. H.; Li, K. H.; Yi, F.; Niu, G. D.; Tang, J. $Cs_2AgInCl_6$ Double Perovskite Single Crystals: Parity Forbidden Transitions and Their Application For Sensitive and Fast UV Photodetectors. *ACS Photonics* **2018**, *5*, 398−405.

(14) Chen, X.; Liu, K.; Zhang, Z.; Wang, C.; Li, B.; Zhao, H.; Zhao, D.; Shen, D. Self-Powered Solar-Blind Photodetector with Fast Response Based on Au/β-Ga_2O_3 Nanowires Array Film Schottky Junction. *ACS Appl. Mater. Interfaces* **2016**, *8*, 4185−4191.

(15) Zhao, B.; Wang, F.; Chen, H.; Zheng, L.; Su, L.; Zhao, D.; Fang, X. An Ultrahigh Responsivity (9.7 mA/W^{-1}) Self-Powered Solar-Blind Photodetector Based on Individual ZnO-Ga_2O_3 Heterostructures. *Adv. Funct. Mater.* **2017**, *27*, 1700264.

(16) Li, X. Y.; Liu, W.; Li, P. G.; Song, J.; An, Y. H.; Shen, J. Q.; Wang, S. L.; Guo, D. Y. A Self-Powered Nano-Photodetector Based on PFH/ZnO Nanorods Organic/Inorganic Heterojunction. *Results Phys.* **2018**, *8*, 468−472.

(17) Wu, Z.; Jiao, L.; Wang, X.; Guo, D.; Li, W.; Li, L.; Huang, F.; Tang, W. A Self-Powered Deep-Ultraviolet Photodetector Based on an Epitaxial Ga_2O_3/Ga:ZnO Heterojunction. *J. Mater. Chem. C* **2017**, *5*, 8688−8693.

(18) Ma, N.; Zhang, K. W.; Yang, Y. Photovoltaic-Pyroelectric Coupled Effect Induced Electricity for Self-Powered Photodetector System. *Adv. Mater.* **2017**, *29*, 1703694.

(19) Bai, F.; Qi, J. J.; Li, F.; Fang, Y. Y.; Han, W. P.; Wu, H. L.; Zhang, Y. A High-Performance Self-Powered Photodetector Based on Monolayer MoS_2/Perovskite Heterostructures. *Adv. Mater. Interfaces* **2018**, *5*, 1701275.

(20) Chen, X.; Xu, Y.; Zhou, D.; Yang, S.; Ren, F. F.; Lu, H.; Tang, K.; Gu, S.; Zhang, R.; Zheng, Y.; Ye, J. Solar-Blind Photodetector with High Avalanche Gains and Bias-Tunable Detecting Functionality Based on Metastable Phase α-Ga_2O_3/ZnO Isotype Heterostructures. *ACS Appl. Mater. Interfaces* **2017**, *9*, 36997−37005.

DOI: 10.1021/acsnano.8b07997
ACS Nano 2018, 12, 12827−12835

(21) Ni, P. N.; Shan, C. X.; Wang, S. P.; Liu, X. Y.; Shen, D. Z. Self-Powered Spectrum-Selective Photodetectors Fabricated from *n*-ZnO/*p*-NiO Core-Shell Nanowire Arrays. *J. Mater. Chem. C* **2013**, *1*, 4445−4449.
(22) Guo, D. Y.; Liu, H.; Li, P. G.; Wu, Z. P.; Wang, S. L.; Cui, C.; Li, C. R.; Tang, W. H. Zero-Power-Consumption Solar-Blind Photodetector Based on β-Ga_2O_3/NSTO Heterojunction. *ACS Appl. Mater. Interfaces* **2017**, *9*, 1619−1628.
(23) Li, P. G.; Shi, H. Z.; Chen, K.; Guo, D. Y.; Cui, W.; Zhi, Y. S.; Wang, S. L.; Wu, Z. P.; Chen, Z. W.; Tang, W. H. Construction of GaN/Ga_2O_3 *p-n* Junction for an Extremely High Responsivity Self-Powered UV Photodetector. *J. Mater. Chem. C* **2017**, *5*, 10562−10570.
(24) Narita, T.; Kachi, T.; Kataoka, K.; Uesugi, T. P-type Doping of GaN by Magnesium Ion Implantation. *Appl. Phys. Express* **2017**, *10*, 016501.
(25) Amano, H. Growth of GaN Layers on Sapphire by Low-Temperature-Deposited Buffer Layers and Realization of *p*-type GaN by Magesium Doping and Electron Beam Irradiation. *Angew. Chem., Int. Ed.* **2015**, *54*, 7764−7769.
(26) Pearton, S. J.; Yang, J. C.; Cary, P. H.; Ren, F.; Kim, J.; Tadjer, M. J.; Mastro, M. A. A Review of Ga_2O_3 Materials, Processing, and Devices. *Appl. Phys. Rev.* **2018**, *5*, 011301.
(27) Guo, D. Y.; Qian, Y. P.; Su, Y. L.; Shi, H. Z.; Li, P. G.; Wu, J. T.; Wang, S. L.; Cui, C.; Tang, W. H. Evidence for the Bias-Driven Migration of Oxygen Vacancies in Amorphous Non-Stoichiometric Gallium Oxide. *AIP Adv.* **2017**, *7*, 065312.
(28) Guo, D. Y.; Qin, X. Y.; Lv, M.; Shi, H. Z.; Su, Y. L.; Yao, G. S.; Wang, S. L.; Li, C. R.; Li, P. G.; Tang, W. H. Decrease of Oxygen Vacancy by Zn-doped for Improving Solar-Blind Photoelectric Performance in β-Ga_2O_3 Thin Films. *Electron. Mater. Lett.* **2017**, *13*, 483−488.
(29) Dong, L. P.; Jia, R. X.; Xin, B.; Peng, B.; Zhang, Y. M. Effects of Oxygen Vacancies on the Structural and Optical Properties of β-Ga_2O_3. *Sci. Rep.* **2017**, *7*, 40160.
(30) Rafique, S.; Han, L.; Neal, A. T.; Mou, S.; Tadjer, M. J.; French, R. H.; Zhao, H. Heteroepitaxy of *N*-type β-Ga_2O_3 Thin Films on Sapphire Substrate by Low Pressure Chemical Vapor Deposition. *Appl. Phys. Lett.* **2016**, *109*, 132103.
(31) Zheng, W.; Huang, F.; Zheng, R.; Wu, H. Low-Dimensional Structure Vacuum-Ultraviolet-Sensitive (λ < 200 nm) Photodetector with Fast-Response Speed Based on High-Quality AlN Micro/Nanowire. *Adv. Mater.* **2015**, *27*, 3921−3927.
(32) Guo, D. Y.; Li, P. G.; Wu, Z. P.; Cui, W.; Zhao, X. L.; Lei, M.; Li, L. H.; Tang, W. H. Inhibition of Unintentional Extra Carriers by Mn Valence Change for High Insulating Devices. *Sci. Rep.* **2016**, *6*, 24190.
(33) Zhao, B.; Wang, F.; Chen, H. Y.; Wang, Y. P.; Jiang, M. M.; Fang, X. S.; Zhao, D. X. Solar-Blind Avalanche Photodetector Based on Single ZnO-Ga_2O_3 Core-Shell Microwire. *Nano Lett.* **2015**, *15*, 3988−3993.
(34) Chen, H.; Yu, P.; Zhang, Z.; Teng, F.; Zheng, L.; Hu, K.; Fang, X. Ultrasensitive Self-Powered Solar-Blind Deep-Ultraviolet Photodetector Based on All-Solid-State Polyaniline/MgZnO Bilayer. *Small* **2016**, *42*, 5809−5816.
(35) Liu, Y. T.; Jia, R. X.; Wang, Y. C.; Hu, Z. Y.; Zhang, Y. M.; Pang, T. Q.; Zhu, Y. J.; Luan, S. Z. Inhibition of Zero Drift in Perovskite-Based Photodetector Devices *via* [6,6]-Phenyl-C61-butyric Acid Methyl Ester Doping. *ACS Appl. Mater. Interfaces* **2017**, *9*, 15638−15643.
(36) Zheng, W.; Zhang, Z. J.; Lin, R. C.; Xu, K.; He, J.; Huang, F. High-Crystalline 2D Layered PbI_2 with Ultrasmooth Surface: Liquid-Phase Synthesis and Application of High-Speed Photon Detection. *Adv. Electron. Mater.* **2016**, *2*, 1600291.
(37) Su, L.; Zhang, Q.; Wu, T.; Chen, M.; Su, Y.; Zhu, Y.; Xiang, R.; Gui, X.; Tang, Z. High-Performance Zero-Bias Ultraviolet Photodetector Based on *p*-GaN/*n*-ZnO Heterojunction. *Appl. Phys. Lett.* **2014**, *105*, 072106.
(38) Fan, M. M.; Liu, K. W.; Chen, X.; Zhang, Z. Z.; Li, B. H.; Shen, D. Z. A Self-Powered Solar-Blind Ultraviolet Photodetector Based on a Ag/ZnMgO/ZnO Structure with Fast Response Speed. *RSC Adv.* **2017**, *7*, 13092−13096.

DOI: 10.1021/acsnano.8b07997
ACS Nano 2018, 12, 12827−12835